Lyophilization of Protein Formulations in Vials: Investigation of the Relationship between Resistance to Vapor Flow during Primary Drying and Small-Scale Product Collapse

DAVID E. OVERCASHIER,* THOMAS W. PATAPOFF, AND CHUNG C. HSU

Contribution from *Department of Pharmaceutical Research and Development, Genentech, Inc., 1 DNA Way, South San Francisco, California 94080.*

Received November 17, 1998. Accepted for publication April 28, 1999.

Abstract □ During the lyophilization process, formulations containing protein, bulking agent, or lyoprotectant form a dry product layer that can affect the transport of sublimed water vapor. We carried out an investigation of the primary drying segment of lyophilization to evaluate the relationship between the resistance to water vapor flow through the dried layer and the microstructure of the dried cake. Recombinant humanized antibody HER2 (rhuMAb HER2) formulated in trehalose was studied, as were protein-free formulations containing trehalose and sucrose. Sublimation rate and product temperature data were used to compute the resistance to mass transfer. Dried cake structure was examined by scanning electron microscopy and a novel fluorescence microscopy method. Collapse temperatures were determined by freeze-drying microscopy. Mass transfer resistance was found to decrease with increases in temperature for each material. Resistance also depended on composition, decreasing in the formulation series, rhuMAb HER2, trehalose, sucrose. The lyophilized material consisted of porous cakes, with a distinct denser region at the top. Formulation and temperature affected the microstructure of the dried cakes. The formulated trehalose and sucrose were seen, by both microscopy techniques, to possess small (2–20 μm) holes in their platelike structures after lyophilization. The quantity of holes was higher for material dried at higher temperature. The collapse temperature (T_c) of a material appeared to play a role in the process, as lower T_c was correlated with lower resistance and a greater extent of holes. Our results are consistent with the theory that lower resistance to water vapor flow in the primary drying stage of lyophilization may be due to small-scale product collapse.

Introduction

Lyophilization is commonly used to prepare protein pharmaceuticals in dry form to extend shelf life. Operating cycles may be several days in length and typically involve three process segments: freezing, primary drying, and secondary drying. Freezing transforms the protein−excipient solution in a vial into two or more phases, usually crystalline ice and an amorphous freeze-concentrate containing the protein, lyoprotectant, and water. Additional phases may also form if the excipient precipitates or crystallizes out during freezing. Primary drying is the sublimation of ice from the frozen vial content under vacuum. Secondary drying, also under vacuum, involves the removal of water from the freeze-concentrate, reducing the residual moisture content to a level (e.g. ≤ 3 wt %/wt) suitable for long-term storage.[1]

* Corresponding author. Tel: (650) 225-3205; fax: (650) 225-3191; e-mail: overcashier.david@gene.com.

In the lyophilization of protein pharmaceuticals, the longest process segment is usually the sublimation of ice from frozen vials. The rate of ice removal is a function of the lyophilizer shelf temperature and chamber pressure.[2−6] The product temperature, which is also dependent on the shelf temperature and the pressure, is often 20−30 °C below that of the shelf as a result of the energy consumed by the transformation of ice to water vapor. The product temperature during primary drying is critical, because too high a temperature can result in product meltback or collapse[7] (potentially degradative events), whereas too low a temperature will result in lengthy lyophilization cycles. The product temperature accompanying a given temperature−pressure combination may vary between formulations.

A key parameter governing the relationship between the independent variables (the lyophilizer's shelf temperature and chamber pressure) and the dependent variables (ice sublimation rate and product temperature) is the resistance to water vapor flow exhibited by the growing dry layer. This layer is composed of the freeze-concentrated protein/excipient solid solution and the voids left after the ice crystals have sublimed. Pikal et al. determined the resistance to vapor flow for potassium chloride, povidone, mannitol, and dobutamine hydrochloride−mannitol solutions using a microbalance with capillary tubes and a method involving pressure measurement inside the vial to characterize vial freeze-drying.[7,8] They demonstrated that the resistance increases with increasing thickness of the dried layer, in a nonlinear fashion. They also reported that the resistance decreases with increasing temperature, a phenomenon ascribed to "hydrodynamic surface flow" of the sublimed water through the pores.

Milton et al. later proposed a different mechanism for the observed temperature dependence of resistance to mass transfer, involving product collapse on a microscopic scale.[9] In that study, the investigators determined the resistance to water vapor flow based on the time-dependent chamber pressure increase during brief interruptions of the flow from the chamber to condenser (by closing a valve between the two). For mannitol, lactose, and potassium chloride solutions, they reported that under some conditions, the resistance to vapor flow increased with thickness of the dried layer, as described above. However, at product temperature values near a material's collapse temperature, the resistance was not affected by increases in thickness. This constant-resistance phenomenon was hypothesized to be due to "microcollapse," the development of additional pathways for vapor flow in the form of holes in the dried material, a proposition supported by SEM photomicrographs of freeze-dried lactose.

Further research on the relationship between temperature, pressure, and sublimation rate was described by Chang and Fischer in their study of lyophilization cycle

10.1021/js980445+ CCC: $18.00
Published on Web 06/09/1999

development for rhIL-1ra formulated at 100 mg/mL.[6] In that study, the authors gave a comprehensive description of product temperatures and sublimation rates resulting from 35 different combinations of shelf temperature and chamber pressure. Unlike the reports described above, they observed the resistance to vapor flow to be independent of product temperature, over a wide range of temperatures (−32 to −14 °C).

This report describes our investigation of primary drying in lyophilization of recombinant humanized antibody HER2 (rhuMAb HER2) formulated in a trehalose−histidine−polysorbate system. This lyophilized product has recently received regulatory approval for breast cancer therapy (based on its capacity to inhibit growth of human breast carcinoma cells[10]). rhuMAb HER2 is formulated at high concentration (relative to other Genentech products), and we believe that the results of our investigation will be useful to others in the field. In this study, we measured sublimation rates and product temperatures for formulated rhuMAb HER2, for a range of lyophilization conditions, and determined mass transfer resistances. In addition, protein-free formulations containing either trehalose or sucrose were studied. Sucrose and trehalose have been shown to stabilize proteins in the dried state,[11−14] i.e., function as "lyoprotectants." The structure of materials after drying was examined by scanning electron microscopy and a newly developed fluorescence microscopy method. This study provided a better understanding of the relationship between resistance to vapor flow and small-scale product collapse in protein lyophilization.

Experimental Section

Materials—rhuMAb HER2, molecular mass approximately 160 kD, was produced at Genentech, Inc. by Chinese hamster ovary cells. It is a glycoprotein of 1328 amino acid residues. The bulk was formulated to contain 25 mg/mL rhuMAb HER2, 20 mg/mL trehalose, 0.1 mg/mL polysorbate 20, and 5 mM histidine, pH 6.0. Two excipient formulations also were tested: 45 mg/mL trehalose, 0.1 mg/mL polysorbate 20, and 5 mM histidine, pH 6.0; and 45 mg/mL sucrose, 0.1 mg/mL polysorbate 20, and 5 mM histidine, pH 6.0. Solutions were prepared in distilled water and 0.2-μm filtered. All components used were reagent grade or better.

Sublimation Rate and Product Temperature Measurement in Vial Freeze-Drying—The sublimation of ice in the formulations of interest was evaluated by carrying out primary drying in Leybold−Heraeus GT20 lyophilizers at constant shelf temperature and chamber pressure. Formulations were filled at 5.0 mL in 10-mL Wheaton tubing glass vials (inner diameter 2.37 cm) with 20-mm neck finish. Vials were stoppered for lyophilization using West gray butyl rubber stoppers. Vials were cooled to −50 °C at 20 °C/h and held for 5 h before proceeding with drying. After the chamber was evacuated to the pressure set point, the lyophilizer shelf was warmed to the temperature set point over a 2-h period. Ice sublimation was allowed to proceed, with constant temperature and pressure set points. Such primary drying tests were conducted at various conditions with the shelf temperatures in the range −20 to +25 °C and the chamber pressure at 100 mTorr (regulated with nitrogen gas). Tests also were carried out at −30 and −35 °C under 50 to 75 mTorr and 25 °C under 200 and 300 mTorr.

The temperature of the vial contents was measured by a 30-gauge Type T thermocouple sensor placed vertically through the vial opening, the tip positioned 1−4 mm above the vial base. For each formulation lyophilized in a run, the product temperature stated is the mean of two to four sensors.

At selected time points throughout primary drying, three preweighed vials of each formulation were stoppered in the chamber using a thief arm installed in the dryer. After lyophilization, the stoppered vials were reweighed to determine the water loss. The sublimation rate was determined from the mean water loss determined at four to six timepoints. It has been reported that a vial adjacent to an empty vial or the edge of the shelf shows a sublimation rate increase of 5% or 20%, respectively, relative to a vial in the middle of an array of subliming vials, presumably due to radiation from the shelf and chamber wall.[3] Thus, in this study only those vials adjacent to equivalent filled vials were sampled for temperature or rate determination.

Determination of Mass Transfer Resistance—The resistance to vapor flow through the dried layer in the vial was determined using a method adapted from the work of Pikal et al.[3,8] In our method, the sublimation rate (essentially time-invariant) and the time-dependent product temperature data were used in order to estimate the product temperature (and the corresponding ice vapor pressure) at the ice sublimation front and the overall mass transfer resistance exhibited by the dried product layer. A brief summary of the pertinent equations is given below.

The overall dried product resistance, $\hat{R}_p$, describes the proportionality between the specific sublimation rate, $\dot{m}/A_p$, and the pressure driving force, $P_o - P_v$:

$$\frac{\dot{m}}{A_p} = \frac{1}{\hat{R}_p} \times (P_o - P_v) \tag{1}$$

where $\dot{m}$ is sublimation rate (g/h), A_p is cross-sectional area of product in the vial (cm^2), $\hat{R}_p$ is normalized dried product resistance (cm^2 mTorr h g^{-1}), P_o is equilibrium vapor pressure of ice at the temperature of the subliming ice (mTorr), and P_v is pressure in the vial (assumed equal to chamber pressure P_c) (mTorr).

In our analysis, we assume that the cross-sectional area of product in the vial, A_p, is equal to the internal area of the vial. Recent work suggests that in certain lyophilization cases this may not be true.[15] The investigators provided some evidence that the sublimation front may be nonplanar (concave down) due to faster drying along the vial wall, following cake shrinkage; for further consideration see the Results and Discussion.

In our application of eq 1, we estimate the pressure in the vial to be approximately equal to the chamber pressure. The substitution of P_c for P_v means that the resistance quantity we determine is the sum, $\hat{R}_p + \hat{R}_s$ (where $\hat{R}_s$ is the resistance to vapor flow exhibited by the stopper). Previous investigators, using modified vials for direct measurement of P_v, reported that the contribution of $\hat{R}_s$ (20-mm stoppers) to the sum ($\hat{R}_p + \hat{R}_s$) was less than 4%[3], supporting our approximation.

The temperature dependence of the ice vapor pressure P_o (mTorr) is given by:[16]

$$P_o = 2.7 \times 10^{13} \times \exp[-6145/(T_i + 273.15)] \tag{2}$$

where T_i is the temperature (°C) of the subliming ice interface.

Inserting the vapor pressure expression (eq 2) in the mass transfer equation (eq 1) and substituting P_c for P_v, we obtain:

$$\frac{\dot{m}}{A_p} = \frac{1}{\hat{R}_p} \times (2.7 \times 10^{13} \times \exp[-6145/(T_i + 273.15)] - P_c) \tag{3}$$

During ice sublimation, heat is supplied by the shelf to the bottom of the vial and is consumed at the sublimation front. The temperature gradient in the ice/solute matrix can be estimated by the Fourier heat conduction model and shown to have the axial length dependence described in eq 4:

$$\frac{dT}{dx} = -\frac{\Delta H_s \times \dot{m}}{A_v \times K_I} \tag{4}$$

where x is the axial position relative to bottom of vial (cm), ΔH_s is the heat of sublimation (cal/g), A_v is the cross-sectional area of vial base (cm^2), and K_I is the thermal conductivity of the product (estimated as the area-weighted sum of thermal conductivities of glass (Wheaton) and ice,[17] as described previously[3]).

By integration of eq 4, we obtain an estimation of the temperature at the subliming ice interface in terms of the measured product temperature (eq 5). The interface can be seen to have the lowest temperature in the vial.

$$T_i = T_p - \frac{\Delta H_s \times \dot{m}}{A_v \times K_I} \times (L - l) \tag{5}$$

where T_p is the product temperature (°C) at the temperature sensor, L is the thickness of product, from temperature sensor to initial fill height (cm), and l is the thickness of dried layer (cm), determined from the interpolated weight loss data, with the assumption that the sublimation front is planar, by the formula $l = (\dot{m} \times t + m_0)/(\rho \times A_v)$, where t is the elapsed time, measured from the time at which the shelf temperature reaches the set point, m_0 is the weight loss at $t = 0$, and ρ is the frozen matrix density.

Uncertainty in the sublimation front temperature, as estimated by eq 5, could result from several sources, including the thermal conductivity of the frozen product in the vial, the relative quantities of radial and axial heat flow, the measured product temperature, the vial geometry, and the shape of the subliming interface. In our experiments, the effect of uncertainty in the thermal conductivity of the frozen product in the vial may be low, due to the use of solutions of constant solute concentration (4.6% w/v) for all tests. The effect of radial heat flow was minimized by surrounding all thermocouple and sublimation rate vials with filled, subliming vials.

The act of measuring product temperature may influence the sublimation process: thermocouple vials may nucleate before "normal" vials, resulting in a different microstructure and, possibly, faster sublimation.[18] In our experiments, the potential effect of thermocouples on microstructure would be constant, independent of drying temperature or formulation composition. Uncertainty in the measured product temperature and in the vial geometry were reduced by using replicate measurements (2−4) for each condition.

We obtain our final equation by substituting eq 5 for the interface temperature term in eq 3 and rearranging:

$$\hat{R}_p = \frac{A_p}{\dot{m}} \times \left(2.7 \times 10^{13} \times \exp\left[\frac{-6145}{T_p - \frac{\Delta H_s \times \dot{m}}{A_v \times K_I} \times (L - l) + 273.15} \right] - P_c \right) \quad (6)$$

Equation 6 allows us to estimate the resistance to mass transfer as a function of the dried layer thickness using the measurable quantities sublimation rate, product temperature, and vial dimensions.

Examination of Dried Cake Structure—The microscopic structure of lyophilized material was evaluated by two methods, scanning electron microscopy (SEM) and a novel fluorescence microscopy technique. Samples to be analyzed were prepared by lyophilization using one of two primary drying conditions, 10 °C, 100 mTorr for 30 h or −30 °C, 70 mTorr for 90 h. Following an increase (at 5 °C/h) in the shelf temperature, secondary drying was conducted at 20 °C, with the pressure unchanged, for 8 h. Vials were stoppered under 720 Torr ± 40 Torr nitrogen and then transferred to a desiccator for further drying. Desiccation over phosphorus pentoxide was initiated at <25 Torr pressure and carried out at 20−25 °C for 7−14 d. Samples for SEM were prepared in a nitrogen-purged glovebox under low (<10%) relative humidity by removing the dried cakes from the vials, sectioning vertically by hand using a single-edge razor blade, mounting to a sample stub, and coating under vacuum with a 10 nm gold−palladium layer. Images were obtained by SEM (Philips model 525M; acceleration 5 kV).

Dried cake structure was also evaluated using a second technique, the fluorescence microscopy of rhodamine-containing "cakes" embedded in wax. To selected vials, rhodamine B aqueous solution (20 μL at 0.5 mg/mL) was added before lyophilization. Solutions were lyophilized and desiccated as described in the previous paragraph. These cakes were then placed under vacuum and heated to 60 °C in the presence of low melting paraffin (The Hygenic Corp., Akron, OH) in which Sudan Black B was dissolved. The melted paraffin was allowed to fill the vial until the entire cake was covered by several millimeters. The vacuum was released, and the vials were cooled to room temperature. The vials were broken carefully and the intact paraffin plugs removed. The paraffin plugs containing the lyophilized cakes were sliced vertically as described above. Images of sections were acquired with a Nikon Optiphot-2 microscope using the filter cube for rhodamine (excitation 510−560 nm, emission > 610 nm). Thermal analysis of the dried material was carried out by differential scanning calorimetry (DSC; Seiko model 120 with model SSC/5200H data station). Samples of approximately 12−20 mg were sealed in Al containers, equilibrated to room temperature, and warmed at 5 °C min^{-1} to 200 °C.

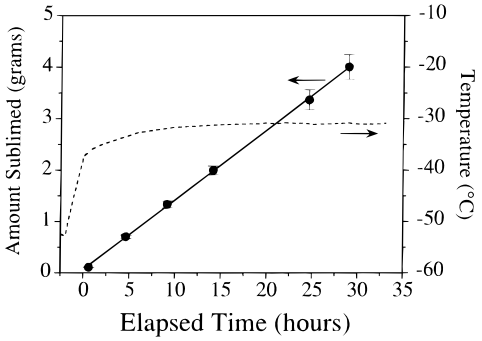

Figure 1—Weight loss (●) and product temperature (- - -) measurements during primary drying of rhuMAb HER2 formulation at –20 °C shelf temperature; 100 mTorr chamber pressure. Note the linearity of the weight loss data.

Collapse Temperature Assessment Using Freeze-Drying Microscope—The presence or absence of collapse during freeze-drying of the rhuMAb HER2, trehalose, and sucrose formulations at various temperatures was investigated using a freeze-drying microscope. This technique was reported by MacKenzie to be useful in identifying structural changes occurring during ice sublimation.[19] In the present study we used a microscope system that includes a compact freeze-drying chamber and a thermoelectric heat pump for cooling. Details of the system were reported previously.[20] The sample to be investigated is held between two glass cover slips on the cooling stage, cooled to approximately −45 °C, and lyophilized as desired.

In our tests, sample freezing was executed in a manner described below to form larger ice crystals for ease of viewing and for faster ice sublimation. A sample aliquot, approximately 4 μL, was cooled to −1.5 °C and held for 1 min to allow for temperature equilibration. The chamber cover was briefly removed, and a dry ice pellet was held against the top glass cover slip for about 5 s to nucleate ice crystals in the sample (at a location away from the microscope viewing area). The sample was held at −1.5 °C for about 2 min and then at −3.5 °C before cooling at 10 °C/min to −45 °C. After a 15-min hold, the chamber was evacuated to approximately 100 mTorr and the stage temperature was increased at 5 °C/min and held at the temperature of interest. It has been shown that the stage temperature and sample temperature are equivalent in this system.[20] The temperature was increased stepwise from −40 °C to −15 °C, in 2−5 °C steps, for each formulation. At the location of the sublimation front, the degree to which the structure of the glassy matrix was retained was evaluated visually. Collapse temperature of the frozen sample was identified as the stage temperature at which the structure was observed to distort or flow. The identification of a collapse temperature is an estimate, since collapse (unlike melting) does not occur at a sharply defined temperature.

Thermal analysis of the frozen aqueous material was carried out using the DSC described above, fitted with a cooling head (mod. CA-5) for controlled cooling by liquid nitrogen. Samples of approximately 15 mg were sealed in Al containers, equilibrated to 5 °C, and cooled at 5 °C min^{-1} to −90 °C. Following equilibration, the sample was warmed at 5 °C min^{-1} to 20 °C.

Results and Discussion

Sublimation Rate and Product Temperature in Vial Freeze-Drying—At a given lyophilizer shelf temperature and pressure, the amount of ice sublimed from vials was approximately linear with respect to time; see Figure 1, depicting rhuMAb HER2 subliming on a −20 °C shelf. Table 1 shows that the sublimation rate was found to increase with higher temperature and pressure set points, as expected. This trend is similar to that reported by

Table 1—Sublimation Rate and Product Temperature for rhuMAb HER2, Trehalose, and Sucrose Formulations (see text) as Functions of Lyophilizer Shelf Temperature and Chamber Pressure

shelf temp (°C)	pressure (mTorr)	specific sublimation rate(g h^{-1} cm^{-2})			product temperature (°C)		
		rhuMAb HER2	trehalose	sucrose	rhuMAb HER2	trehalose	sucrose
25	300	0.19			–20		
25	200	0.16	0.15		–21	–28	
25	100	0.11	0.13		–26	–30	
10	100	0.084	0.083	0.098	–26	–30	–34
–20	100	0.031	0.031	0.035	–31	–36	–37
–30	70			0.019			–37
–30	50	0.014	0.015		–37	–37	
–35	75		0.011	0.012		–37	–37

others.[2–6] The data also indicate that under the same shelf temperature and chamber pressure conditions, sublimation rates for all formulations were approximately equal, except for two conditions at which sucrose rates were slightly higher. The rates reported in Table 1 have coefficients of variation (defined as the standard error divided by the mean) of 1.2 to 3.4%.

During each run, the product temperature was observed to increase as the shelf temperature was ramped from −50 °C to the primary drying shelf temperature set point, then level off (Figure 1). The product temperature was sensitive to shelf temperature, chamber pressure, and formulation (Table 1; data correspond to the middle portion of the sublimation process, at which time the product temperature was approximately constant). The product temperatures during primary drying followed the formulation series, rhuMAb HER2 > trehalose > sucrose, at most process conditions. It might be expected that product temperature and sublimation rate are connected, yet under some process conditions we observed differences in product temperatures between formulations, even though the sublimation rates were approximately equivalent. This situation may be due to differences between formulations in resistance to vapor flow, as is discussed below.

Determination of Mass Transfer Resistance—The measured resistance to mass transfer was seen to increase with increased dry layer thickness (Figure 2; rhuMAb HER2, −20 °C temperature), as expected. The thickness dependence gave a good fit to the nonlinear model proposed by Pikal et al.[8] and shown in eq 7:

$$\hat{R}_p = \frac{A_0 + A_1 l}{1 + A_2 l} \qquad (7)$$

where A_0, A_1, A_2 are constants determined from fitting of data. Figure 2 also illustrates the increase in resistance to vapor flow per unit thickness ($d\hat{R}_p/dl$). As reported previously,[8] the derivative function was high at low values of dried layer thickness and low at higher thicknesses, suggesting that a denser layer was present at the top of the vial.

Figure 3 shows the resistance to mass transfer determined for ice sublimation in the rhuMAb HER2 formulation at several temperature and pressure set points. The mass transfer resistance was sensitive to the shelf temperature, with higher resistance values shown by material processed at lower temperatures. This functionality was reported previously,[8,9] as described above.

Mass transfer resistance was also determined for formulated trehalose (Figure 4) and sucrose (Figure 5). These materials showed similar effects of thickness and shelf temperature on resistance as those seen with rhuMAb HER2. However, the resistance to mass transfer was lower, under most conditions, for trehalose than for rhuMAb HER2, and the resistance for the sucrose-containing material was lower still. Only at lower shelf temperatures (−30 and −35 °C) did the three materials appear equivalent.

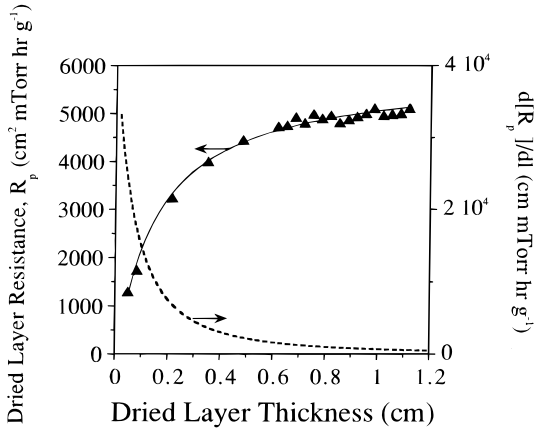

Figure 2—Resistance to mass transfer, $\hat{R}_p$, as a function of dried layer thickness for rhuMAb HER2 at –20 °C, 100 mTorr (▲). The equation for the $\hat{R}_p$ curve fit (solid line) is described in the text (eq 7). Also shown is the derivative (dotted line) of the curve fit, representing the increase in resistance as a function of the increase in dried layer thickness. The derivative curve shows that the upper layer of the dried cake contributes more to the resistance than does the lower portion, suggesting a nonuniformity in the dried layer with respect to vertical position.

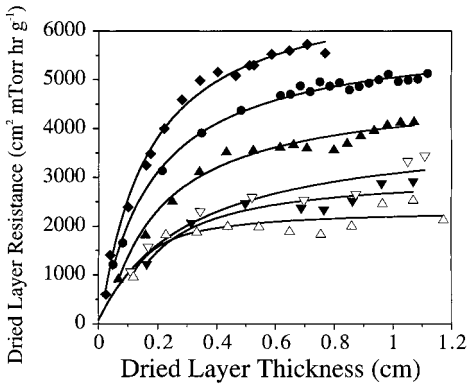

Figure 3—Resistance to mass transfer as a function of dried layer thickness for rhuMAb HER2 at a variety of processing conditions (pressure = 100 mTorr unless noted): –30 °C/50 mTorr (◆), –20 °C (●), 10 °C (▲), 25 °C (▼), 25 °C/200 mTorr (▽), 25 °C/300 mTorr (△). Higher temperature and pressure were observed to result in lower resistance.

The relationships between vapor transfer resistance and temperature at the ice−dry layer interface, determined at the dry layer thickness $l = 0.8$ cm, are summarized for the three formulations in Figure 6. These measurements yield "snapshots" of the ice sublimation processes at points at which approximately 70% of the material had sublimed, enabling the examination of mass transfer resistance as functions of formulation and temperature. The resistance followed the series rhuMAb HER2 > trehalose > sucrose,

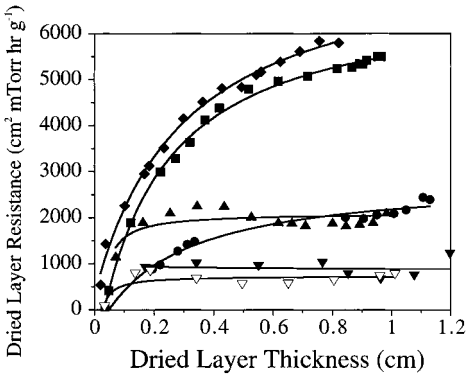

Figure 4—Resistance to mass transfer as a function of dried layer thickness for formulated trehalose at a variety of processing conditions (pressure = 100 mTorr unless noted): –35 °C/75 mTorr (■), –30 °C/50 mTorr (◆), –20 °C (●), 10 °C (▲), 25 °C (▼), 25 °C/200 mTorr (▽). Resistance generally decreased with increased temperature and pressure and was lower at most conditions than that observed for formulated rhuMAb HER2 (Figure 3).

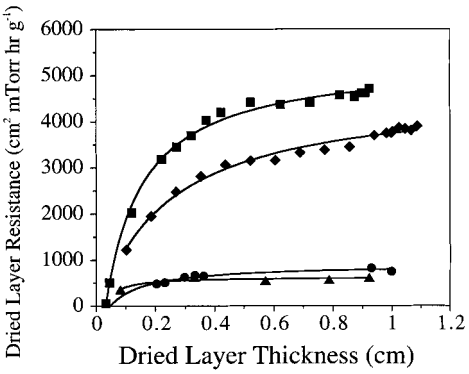

Figure 5—Resistance to mass transfer as a function of dried layer thickness for formulated sucrose at a variety of processing conditions (pressure = 100 mTorr unless noted): –35 °C, 75 mTorr (■), –30 °C, 70 mTorr (◆), –20 °C (●), 10 °C (▲). Resistance decreased with increased temperature and pressure and was lower than that observed for the rhuMAb HER2 (Figure 3) and trehalose (Figure 4) formulations.

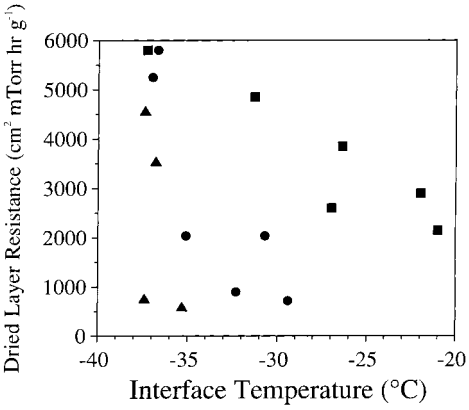

Figure 6—Mass transfer resistance for formulated rhuMAb HER2 (■), trehalose (●), and sucrose (▲) vs interface temperature. Data shown represent values at a dried layer thickness of 0.8 cm. Resistance followed the series rhuMAb HER2 > trehalose > sucrose and decreased with increased interface temperature.

except at interface temperatures below −36 °C, for which the resistances were approximately equal. Figure 6 also illustrates the decrease in resistance with increased temperature. The temperature sensitivity of resistance was highest for sucrose and lowest for rhuMAb HER2.

It is interesting to note that, even under operation conditions which showed large differences between formulations in mass transfer resistance (e.g., 45−80%), the differences in sublimation rate were moderate (8−17%). Limitations in the transfer of heat from the lyophilizer shelf to the vial may be responsible for this phenomenon, although its study was beyond the scope of this work.

As described above, some investigators have hypothesized that when cake shrinkage occurs in lyophilization, the sublimation front may be nonplanar (the magnitude of deviation from a planar sublimation front is not described).[15] In our study, slight shrinkage was observed, so the mass transfer resistance values we determined may be affected by the hypothesized nonplanar nature of the subliming interface. One might expect that the impact of a nonplanar interface would be minimized by the study of relatively thin, flat sections of material. In our study, we monitored the sublimation of 0.8 to 1.0 cm material (average thickness) in vials of diameter 2.4 cm. The effect of nonplanarity, therefore, may have been small. The formulations evaluated in this study exhibited similar cake shrinkage during lyophilization, so the shape of the subliming interface (if not planar) may have been independent of the formulation and drying conditions which we compared.

Overall, uncertainty in the mass transfer resistance results from variability in the measured parameters. In our study, the highest observed uncertainty in sublimation rate (C.V.) was 3.4%; the variation between replicate product temperature values (standard deviation) was 0.1 to 0.8 °C. Analysis of eq 6 shows that "worst-case" errors in rate and temperature have the following effects: An error of ±10% in the sublimation rate gives rise to a variation in mass transfer resistance of ±10%; uncertainty in product temperature of 1 °C induces a variation in resistance of ±20%. These errors in the calculated resistance, while not insignificant, are less than the magnitude of differences between temperatures and formulations shown.

Examination of Dried Cake Structure—The dried material produced by the two lyophilization cycles tested formed white, porous cakes showing slight shrinkage; no large-scale collapse was observed. The morphology of lyophilized material was observed using two techniques, fluorescence microscopy of wax embedded cakes and SEM. The fluorescence images revealed the dried material to have a microporous structure, with a distinct denser layer at the top of the cake (Figure 7A; rhuMAb HER2 dried with a 10 °C primary drying shelf temperature). Examination of this layer at higher magnification (not shown) revealed the layer to have fewer, smaller channels relative to the rest of the dried cake. The layer may contribute to the high $d\hat{R}_p/dl$ corresponding to low dry layer thicknesses, as described above.

At a smaller scale, SEM showed that lyophilization of formulated rhuMAb HER2 using a 10 °C primary drying shelf temperature produced a smooth, platelike structure built around the pores left by the sublimed ice (Figure 7B). The fluorescence microscopy method also illustrated a structure composed of smooth plates and channels (Figure 7C). Formulated rhuMAb HER2 prepared by a −30 °C primary drying shelf temperature was seen, by both methods, to have a similar appearance (not shown).

Lyophilization of formulated trehalose gave a structure which, like rhuMAb HER2, was composed of plates but also contained holes approximately 2−8 μm in diameter. These holes are illustrated by SEM for the 10 °C (Figure 8A) and −30 °C (Figure 8B) primary drying conditions, with lower temperature giving smaller and fewer holes. Holes were also detected by the fluorescence microscopy technique (Figure 8C; 10 °C). As with SEM, fluorescence microscopy detected fewer holes for the −30 °C process (not shown) than for the 10 °C version. Holes of this size range were also reported by others in the lyophilization of lactose.[9]

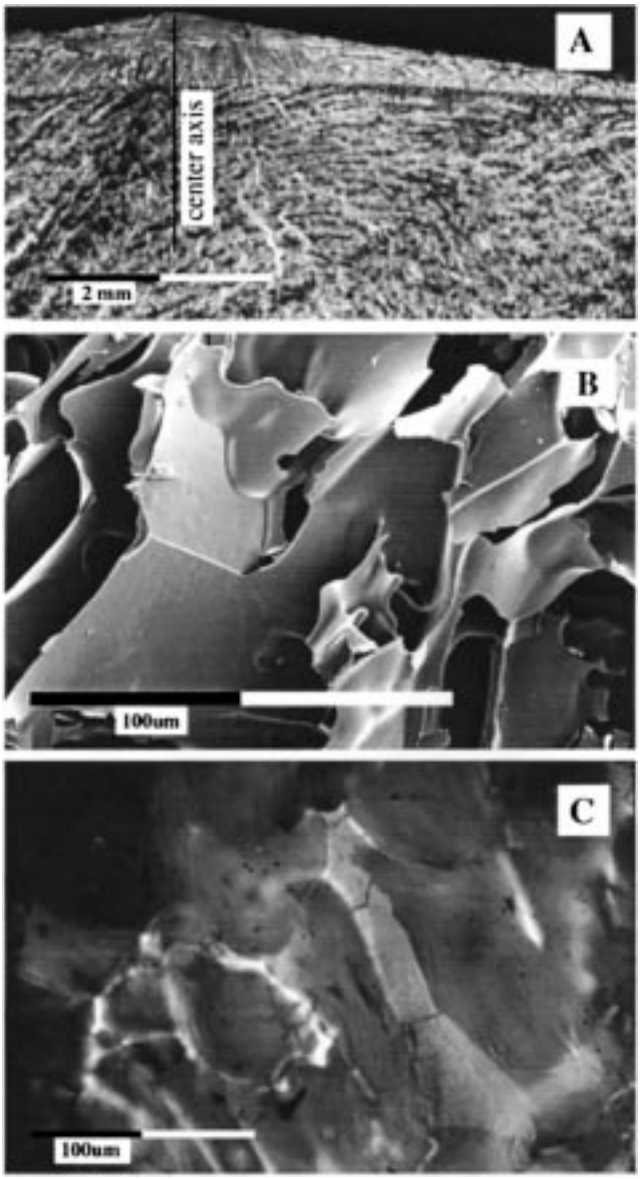

Figure 7—Structure of lyophilized rhuMAb HER2 formulation (10 °C primary drying shelf temperature). (A) Note the denser layer present at the top. The denser layer may be responsible for the higher resistance per unit thickness corresponding to low dried layer thicknesses (Figures 2–5). Fluorescence microscopy, 8X magnification. (B) Note the smooth, plate-like features, separated by open pores. SEM, 270X magnification. (C) Note the smooth structure. Fluorescence microscopy, 150X magnification.

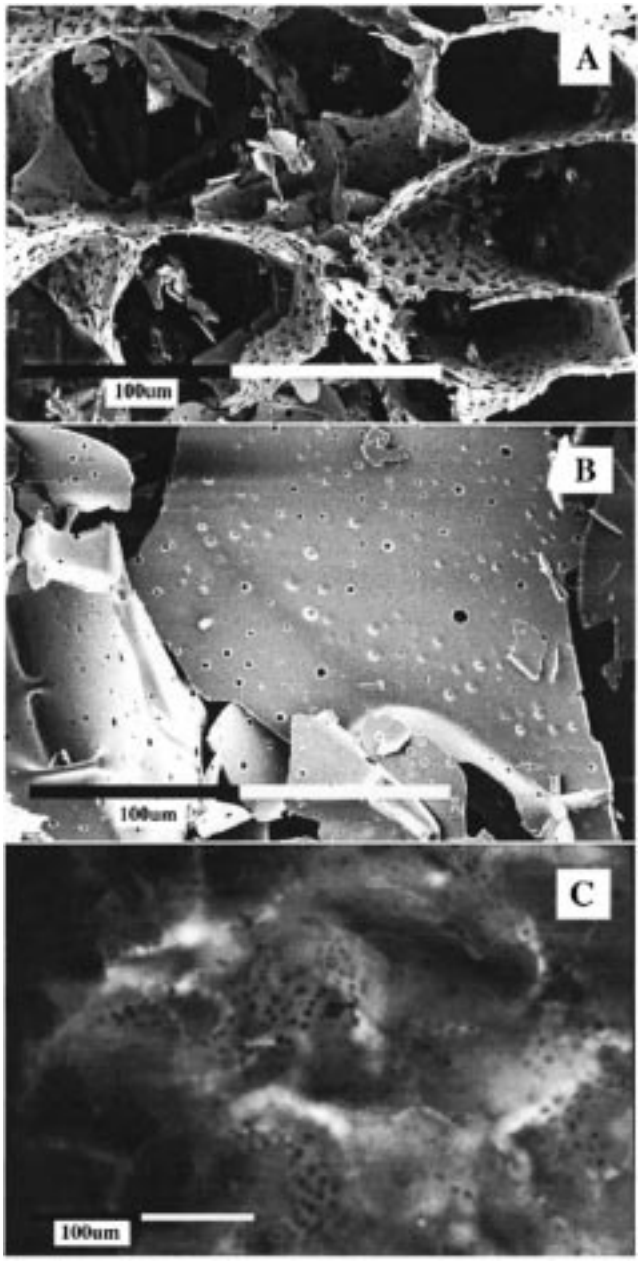

Figure 8—Structure of lyophilized trehalose formulation. Note the appearance of small holes (diameter ~2–8 μm) in the "plates." (A) 10 °C shelf: The large pores (diameter ~100 μm) are thought to be established when the ice crystals grew into the freeze-concentrate. SEM, 270X magnification. (B) –30 °C shelf: The holes are smaller and fewer than those observed in formulated trehalose prepared at the 10 °C shelf temperature. SEM, 270X magnification. (C) 10 °C shelf: Fluorescence microscopy, 150X magnification.

Interestingly, Figure 8A illustrates the pores, approximately 100 μm in diameter, formed by the ice crystals and providing the main avenue for vapor flow through the dried product layer.

The sucrose formulation was seen by SEM to possess holes in the dried structure, both for the 10 °C (Figure 9) and −30 °C process conditions. In addition, the sucrose structures were more "rounded" than the other formulations, with an appearance (Figure 9) suggesting viscous flow of the freeze-concentrate. As with the trehalose formulation, the lower temperature process gave fewer, smaller holes (not shown). Fluorescence microscopy also detected holes in the lyophilized sucrose from both the 10 °C and −30 °C processes (not shown).

The images acquired using the two microscopy techniques indicate that the structure of dried material is sensitive to composition and to the drying process used. Microscopy indicates that the formulated rhuMAb HER2 dries into intact plates, whereas the trehalose and sucrose formulations develop holes in the structure. These holes are more prevalent in material dried by the higher primary drying shelf temperature, so it is likely that they are produced during primary drying. The extent of holes observed in the structure of dried material, increasing with temperature and also in the formulation sequence rhuMAb HER2−trehalose−sucrose, is correlated with lower mass transfer resistance. This agreement suggests that the holes can be an important contributor to the conductance of water vapor through the dried layer. The gradual decrease in mass transfer resistance as a function of temperature seen for rhuMAb HER2 (in the absence of observed holes) suggests that other factors may also play a role.

DSC analysis of the material prepared for microscopic evaluation showed glass transition temperatures (T_g) of 76

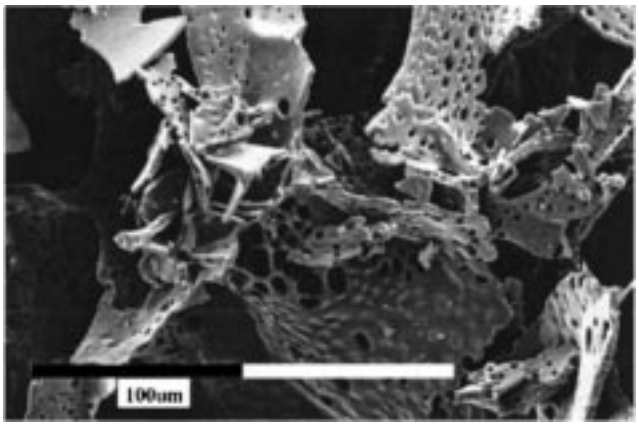

Figure 9—Structure of lyophilized sucrose formulation (10 °C shelf). Note the appearance of small holes (diameter 2–20 μm) in the "plates." Larger holes and smoothed structure suggests increased material flow over that seen in the rhuMAb HER2 and trehalose formulations. SEM, 270X magnification.

Table 2—Transition Temperatures for Frozen Aqueous Formulations Determined by Freeze-Drying Microscopy and DSC

	freeze-drying microscope		DSC: phase transition temp (°C)
formulation[a]	collapse temp (°C)	comment	
rhuMAb HER2	–20	"liquid" phase very viscous	–22
trehalose	–34		–38, –30
sucrose	–40	"liquid" phase flows readily	–43, –33

[a] The composition of each formulation is described in the text.

°C for the sucrose formulation and over 110 °C for the rhuMAb HER2 and trehalose formulations (data not shown). The high T_g values suggest that the materials were thermally stable at the conditions used in the sample preparation and microscopic analysis. In addition, similar structural characteristics were observed by the two methods of microscopy, suggesting that the structures observed were not induced by the evaluation methods. Although the resolution of the fluorescence microscopy technique is lower than that of SEM, it is sufficient to show the presence or absence of holes in the cake structure. In addition, the wax embedment involved in the fluorescence microscopy technique may be useful in protecting samples from atmospheric moisture. This method is under investigation in other freeze-drying studies.

Collapse Temperature Assessment Using Freeze-Drying Microscope—The frozen sample, as observed in the freeze-drying microscope, was composed of branched ice crystals separated by thinner freeze-concentrate regions. Ice crystal growth during cooling was generally from the nucleation site at the center of the stage toward the edges of the sample. Upon evacuation of the chamber, ice sublimation was observed to take place from the edge toward the center of the sample. For each formulation, the structure of the freeze-concentrate was retained at the ice sublimation front at lower stage temperatures but was lost at higher temperatures, as the freeze-concentrated material achieved greater mobility.

The approximate collapse temperature (T_c) and phase transition temperatures (obtained by DSC) for formulated rhuMAb HER2, trehalose, and sucrose are given in Table 2. The formulated rhuMAb HER2 gave the highest T_c, while the sucrose formulation gave the lowest T_c. In our tests, a solution of neat sucrose gave a collapse temperature of −31 to −32 °C, which matches the value reported previously by MacKenzie, −32 °C.[19] For the two protein-free formulations, DSC showed two transitions, possibly corresponding to the glass transition and collapse phenomena. The DSC phase transition temperatures are similar to the T_c data and show the same formulation dependence; we emphasize the T_c results because of their connection to ice sublimation.

For the formulations tested, lower T_c was correlated with lower mass transfer resistance (Figure 6). The data in Table 2 and Figure 6 also suggest that there may be a relationship, for each formulation, between T_c and the temperature dependence of resistance.

The mass transfer resistance data, structure observed by the two microscopy techniques, and collapse temperature results provide a consistent description of ice sublimation and water vapor transport through the dried layer. Increased product temperature during primary drying resulted in lower resistance to vapor flow and, in some cases, the formation of the holes in the dried cake. Between formulations, lower collapse temperature was correlated with lower resistance and more holes. These observations support the theory, set forth by Milton et al. and supported with data for lactose lyophilization,[9] that the alteration in material structure accompanying small-scale collapse results in decreased resistance to water vapor flow in primary drying.

Conclusions

The resistance to water vapor flow through the dried cake layer, as determined from ice sublimation rate and product temperature data, was observed to decrease with increases in temperature. Resistance was also found to depend on formulation, with values following the series: rhuMAb HER2 > trehalose > sucrose. At many process conditions, different formulations were observed to have similar sublimation rates but differing product temperatures. Mass transfer resistance variation between formulations appears to account for these differences. The structure of the dried cake was evaluated by SEM as well as with a newly developed fluorescence microscopy technique. The presence of a dense layer at the top of the dried cake, which may be responsible for the higher resistance determined for this region, was observed. Temperature and formulation affected the microstructure of the cakes. Some of the formulations tested were found to possess small (2−20 μm) holes in their structure after lyophilization. The extent of the holes was observed to increase with the processing temperature, as well as in the formulation series, rhuMAb HER2−trehalose−sucrose. The collapse temperature (T_c), determined by freeze-drying microscopy, was found to decrease over the same formulation series. For the materials studied, lower resistance was correlated with a greater extent of holes and lower T_c. The data obtained in this study support the view that lower resistance to water vapor flow in the primary drying stage of lyophilization may be the result of small-scale product collapse.

References and Notes

1. Pikal, M. J.; Dellerman, K.; Roy, M. L. Formulation and Stability of Freeze-dried Proteins: Effects of Moisture and Oxygen on the Stability of Freeze-dried Formulations of Human Growth Hormone. In *International Symposium on Biological Product Freeze-Drying and Formulation*; May, J. C., Brown, F., Eds.; Karger: Basel, 1991; Vol. 74, pp 21−38.
2. Nail, S. L. The Effect of Chamber Pressure on Heat Transfer in the Freeze-Drying of Parenteral Solutions. *J. Parenter. Drug Assoc.* **1980**, *34*, 358−368.
3. Pikal, M. J.; Roy, M. L.; Shah, S. Mass and Heat Transfer in Vial Freeze-Drying of Pharmaceuticals: Role of the Vial. *J. Pharm. Sci.* **1984**, *73*, 1224−1237.
4. Livesey, R. G.; Rowe, T. W. G. A Discussion of the Effect of Chamber Pressure on Heat and Mass Transfer in Freeze-Drying. *J. Parenter. Sci. Technol.* **1987**, *41*, 169−171.

5. Pikal, M. J.; Shah, S. The Collapse Temperature in Freeze-Drying: Dependence on Measurement Methodology and Rate of Water Removal from the Glassy Phase. *Int. J. Pharm.* **1990**, *62*, 165−186.
6. Chang, B. S.; Fischer, N. L. Development of an Efficient Single-Step Freeze-Drying Cycle for Protein Formulations. *Pharm. Res.* **1995**, *12*, 831−837.
7. Pikal, M. J. Use of Laboratory Data in Freeze-Drying Process Design: Heat and Mass Transfer Coefficients and the Computer Simulation of Freeze-Drying. *J. Parenter. Sci. Technol.* **1985**, *39*, 115−139.
8. Pikal, M. J.; Shah, S.; Senior, D.; Lang, J. E. Physical Chemistry of Freeze-Drying: Measurement of Sublimation Rates for Frozen Aqueous Solutions by a Microbalance Technique. *J. Pharm. Sci.* **1983**, *72*, 635−650.
9. Milton, N.; Pikal, M. J.; Roy, M. L.; Nail, S. L. Evaluation of Manometric Temperature Measurement as a Method of Monitoring Product Temperature During Lyophilization. *PDA J. Pharm. Sci. Technol.* **1997**, *51*, 7−16.
10. Fendly, B. M.; Winget, M.; Hudziak, R. M.; Lipari, M. T.; Napier, M. A.; Ullrich, A. Characterization of Murine Monoclonal Antibodies Reactive to Either the Human Epidermal Growth Factor Receptor or HER2/neu Gene Product. *Cancer Res.* **1990**, *50*, 1550−1558.
11. Townsend, M. W.; DeLuca, P. P. Use of Lyoprotectants in the Freeze-Drying of a Model Protein, Ribonuclease A. *J. Parenter. Sci. Technol.* **1988**, *42*, 190−199.
12. Carpenter, J. F.; Crowe, J. H. An Infrared Spectroscopic Study of the Interactions of Carbohydrates with Dried Proteins. *Biochemistry* **1989**, *28*, 3916−3922.
13. Prestrelski, S. J.; Pikal, K. A.; Arakawa, T. Optimization of Lyophilization Conditions for Recombinant Human Interleukin-2 by Dried-State Conformational Analysis Using Fourier Transform Infrared Spectroscopy. *Pharm. Res.* **1995**, *12*, 1250−1259.
14. Crowe, L. M.; Reid, D. S.; Crowe, J. H. Is Trehalose Special for Preserving Dry Biomaterials? *Biophys. J.* **1996**, *71*, 2087−2093.
15. Pikal, M. J.; Shah, S. Intravial Distribution of Moisture During the Secondary Drying Stage of Freeze-Drying. *PDA J. Pharm. Sci. Technol.* **1997**, *51*, 17−24.
16. Jansco, G.; Pupezin, J.; Van Hook, W. A. The Vapor Pressure of Ice Between 0.01 and −100 °C. *J. Phys. Chem.* **1970**, *74*, 2984−2989.
17. Fletcher, N. H. *The Chemical Physics of Ice*; Cambridge University Press: London, 1970, p 143.
18. Roy, M. L.; Pikal, M. J. Process Control in Freeze-Drying: Determination of the End Point of Sublimation Drying by an Electronic Moisture Sensor. *J. Parenter. Sci. Technol.* **1989**, *43*, 60−66.
19. MacKenzie, A. P. Collapse During Freeze-Drying − Qualitative and Quantitative Aspects. In *Freeze-Drying and Advanced Food Technology*; Goldblith, S. A., Rey, L., and Rothmayr, W. W., Eds.; Academic Press: London, 1975; pp 277−307.
20. Hsu, C. C.; Walsh, A. J.; Nguyen, H. M.; Overcashier, D. E.; Koning-Bastiaan, H.; Bailey, R. C.; Nail, S. L. Design and Application of a Low-Temperature Peltier-Cooling Microscope Stage. *J. Pharm. Sci.* **1996**, *85*, 70−74.

Acknowledgments

We thank Kin Sit, Mary Cromwell, Jamie Moore, Phuong-Anh Nguyen, Al Stern, and Janet Curley for technical assistance and Dr. Tue Nguyen for support of this study.

JS980445+